Truly Combining the advantages of polymeric and zeolite membranes for gas separations

Authors: Xiaoyu Tan[1], Sven Robijns[2], Raymond Thür[1]†, Quanli Ke[2]‡, Niels De Witte[3], Aran Lamaire[4], Yun Li[1], Imran Aslam[1], Daan Van Havere[1], Thibaut Donckels[2], Tom Van Assche[3], Veronique Van Speybroeck[4], Michiel Dusselier[2]*, Ivo Vankelecom[1]*

Affiliations:

[1]Centre for Membrane Separations, Adsorption, Catalysis and Spectroscopy for Sustainable Solutions (cMACS), KU Leuven; Celestijnenlaan 200F, Leuven, 3001, Belgium.

[2]Center for Sustainable Catalysis and Engineering, KU Leuven; Celestijnenlaan 200F, Leuven, 3001, Belgium.

[3]Department of Chemical Engineering, Vrije Universiteit Brussel; Pleinlaan 2, Brussels, 1050, Belgium.

[4]Center for Molecular Modeling, Ghent University; Tech Lane Ghent Science Park, Technologiepark 46, Zwijnaarde, 9052, Belgium.

†Present address: Agfa-Gevaert NV; Septestraat 27, Mortsel, 2640, Belgium.

‡Present address: Institute of Catalytic Reaction Engineering, Zhejiang University of Technology; Hangzhou, 310014, China.

*Corresponding author. Email: ivo.vankelecom@kuleuven.be; michiel.dusselier@kuleuven.be

Abstract: Mixed matrix membranes (MMMs) have been investigated to render energy-intensive separations more efficiently by combining the selectivity/permeability performance, robustness and non-ageing properties of the filler with the easy processing, handling and scaling-up of the polymer. Herein, we fill a commercial polyimide with ultra-high loadings of a high-aspect-ratio, CO_2-philic Na-SSZ-39 zeolite with 3D-channel system that precisely separates gas molecules. By carefully designing both zeolite and MMM synthesis, a gas-permeation highway was created across the flexible membrane. The ageing-resistant (~1 year test) combination of a CO_2/CH_4 mixed gas selectivity ~423 and a CO_2 permeability ~8300 Barrer) outperforms all existing polymer-based membranes and even zeolite-only counterparts.

One-Sentence Summary: A well-designed zeolite-filled mixed matrix membrane outperforms zeolite-only membranes in gas separation.

Over the past decades, membrane technology has matured into an established technology for many energy-intensive separations (*1-3*). Compared to conventional technologies, membrane technology offers a more sustainable alternative, owing to its low-energy consumption, small footprint and modular design, making it possible to retrofit membranes in existing plants (*2*, *3*). Membranes are already in use for gas separations, e.g. natural gas purification, syngas treatment and air separation (*4-7*), and are becoming part of the toolbox for CO_2 removal (*5-10*). Whereas conventional polymeric membranes are cheap and processable, they often suffer from ageing issues or an intrinsic permeability/selectivity trade-off which makes it challenging to obtain high permeability together with sufficient selectivity (*11–16*). On the other hand, inorganic membranes prepared from zeolites and other crystalline microporous materials, like metal-organic frameworks (MOFs), typically display better separation performances but tend to be brittle and more expensive, and possess poor processability and scalability (*17–21*). Mixed-matrix membranes (MMMs), consisting of fillers embedded in a polymeric matrix, aim at combining the intrinsic advantages of a polymeric membrane with the filler's superior gas separation properties (*22–27*).

Zeolites are of particular interest for MMM development as they have well-defined, rigid pores and outstanding thermal and chemical stability. Since the intrinsically low selectivity and high permeability of rubbery polymers (e.g. polydimethylsiloxane) neutralize the benefits of the zeolite, rigid glassy polymers are key to develop high-performance zeolite-filled MMMs (*28–32*). However, the poor adhesion between zeolites and glassy polymers typically results in non-selective interfacial voids (*31*, *32*). Consequently, obtaining high zeolite loadings (≥50 wt.%) while guaranteeing a defect-free polymer-zeolite interface in combination with a highly selective zeolite and appropriate glassy polymer matrix is essential to create high-performance MMMs for a variety of the most critical separation challenges. In this work, a platelet-shaped, CO_2-philic, small pore (8-membered-ring) AEI-type zeolite (SSZ-39) (*33–36*), possessing a long-range ordered 3D-channel system and gas-selective windows is incorporated in a poly(3,3′-4,4′-benzophenone tetracarboxylic-dianhydride diaminophenylindane) (Matrimid® 5218) polymer. Thanks to the combination of well-designed zeolite and MMM synthesis, we obtain a high zeolite loadings with a quasi-continuous zeolite phase across a self-standing membrane

Result and discussion

Zeolite characterization

SSZ-39 zeolites were synthesized according to modified literature recipes (*33–35*). X-ray diffraction (XRD) of the samples confirmed the highly-crystalline, pure AEI type zeolite (Fig. S9). N_2 physisorption demonstrated a micropore volume of ~0.3 cm^3/g (Fig. S11), close to the theoretical accessible volume of the AEI-type framework (*37*), suggesting a nearly-perfect 3D-connected channel system, allowing fast gas transport. TEM images showed platelet-shaped SSZ-39 particles (Fig. 1A) of ~150 nm thickness and ~1.8×1.8 μm^2 in size (Fig. S48); the average aspect-ratio thus reaching ~12. The random packing of the high-aspect-ratio zeolite platelets (Fig. S49) results in a low bulk density of ~15 mg/cm^3 (Fig. S12), while elemental analysis of the as-synthesized SSZ-39 indicated a Si/Al molar ratio of ~11 (Table S3).

CO_2, CH_4 and N_2 uptake and isosteric adsorption enthalpies (Q_{st}) were determined for both calcined SSZ-39 (Na/Al ratio ≈ 0.12) and Na^+-exchanged SSZ-39 (Na-SSZ-39, Na/Al ratio ≈ 0.93) (Table S3). The adsorption isotherms of CO_2, CH_4 and N_2 at 10 °C are shown in Fig. 1D for a pressure range of 0-8 bar. The theoretical maximum CO_2 uptake of Na-SSZ-39 reached ~7.0 mmol/g (~11.0 mmol/cm^3) at 10 ºC, and the steric heat of adsorption for CO_2 at zero coverage was -35.1 kJ/mol, reflecting a desired strong physical adsorption for membrane applications. For both

SSZ-39 and Na-SSZ-39, the gas uptake decreases in the order $CO_2 \gg CH_4 > N_2$. The isosteric adsorption enthalpy of CO_2 in Na-SSZ-39 was far larger than that of CH_4 (-21.4 kJ/mol) and N_2 (-19.4 kJ/mol) as a result of the large polarizability and quadrupole moment of CO_2 (*38*). A more negative CO_2 adsorption enthalpy was obtained on Na-SSZ-39 compared to SSZ-39 (Table S19). Additionally, the pronounced difference in CO_2 adsorption in the low pressure region of the isotherms (Fig. 1D), suggests that Na^+-exchange resulted in an increased CO_2-philicity (*38*).

To better understand these findings at a molecular level, the pure-gas and mixed-gas adsorption behavior in Na-SSZ-39 were modelled using Grand Canonical Monte Carlo (GCMC) simulations. The pure-gas adsorption simulations show a good qualitative resemblance with the experimental data (Fig. S37) and the enthalpies of adsorption are in good agreement (at 2 bar, GCMC yields -31.6 kJ/mol for CO_2, -18.5 kJ/mol for CH_4, -15.8 kJ/mol for N_2). The 3D density iso-surfaces for CO_2 adsorption (Fig. 1C) show that CO_2 molecules preferentially interact with the Na^+ (especially at low CO_2 pressures), while the windows of Na-SSZ-39 remain open for gas transport. This tendency corroborates the enhanced CO_2-philicity by Na^+-exchange, improving CO_2 adsorption/transport in Na-SSZ-39. The Si/Al molar ratio of 11 implies that, on average, one aluminum-site (fully counted) and thus one sodium ion exists per cage (*37*). Furthermore, the CO_2/CH_4 and CO_2/N_2 mixed-gas sorption simulations demonstrate the competitive sorption of CO_2 at the expense of CH_4 and N_2 (Movie S1). This strong competitive sorption behavior drastically reduces the uptake of CH_4 and N_2. For instance, compared to the single-gas adsorption, the CH_4 uptake from an equimolar CO_2/CH_4 mixture was reduced by 88.7% (for N_2, 93.3%) at 10 bar/25 °C (Fig. 1E and 1F). In addition, *ab-initio* free energy barrier calculations (using enhanced sampling molecular dynamics (MD) simulations) for the diffusion inside the zeolite confirmed the molecular sieving behavior of Na-SSZ-39 (Fig. S41). The biggest (static) aperture of Na-SSZ-39 predicts diffusion of molecules with a diameter of 3.84 Å, which is close to the kinetic diameter of CH_4 (3.80 Å) but prominently larger than CO_2 (3.30 Å). Consequently, the free energy barrier for CH_4 permeation through the 8-membered-ring in Na-SSZ-39 is far higher than for CO_2 (a 18.7 kJ/mol difference). Therefore, the self-diffusion coefficient for CO_2 is ~1000-fold larger than for CH_4. Consequently, in a CO_2/CH_4 mixture, CH_4 is prevented from entering the zeolite by a geometric restriction supplemented by a competitive advantage in CO_2 adsorption. By combining the results of MD and GCMC simulations, the theoretical CO_2/CH_4 mixture gas selectivity in Na-SSZ-39 zeolite mounted to >10000 (at 25 °C), thus pointing towards a substantial potential for further improving membrane performance based on this outstanding zeolite platform (more details in SI).

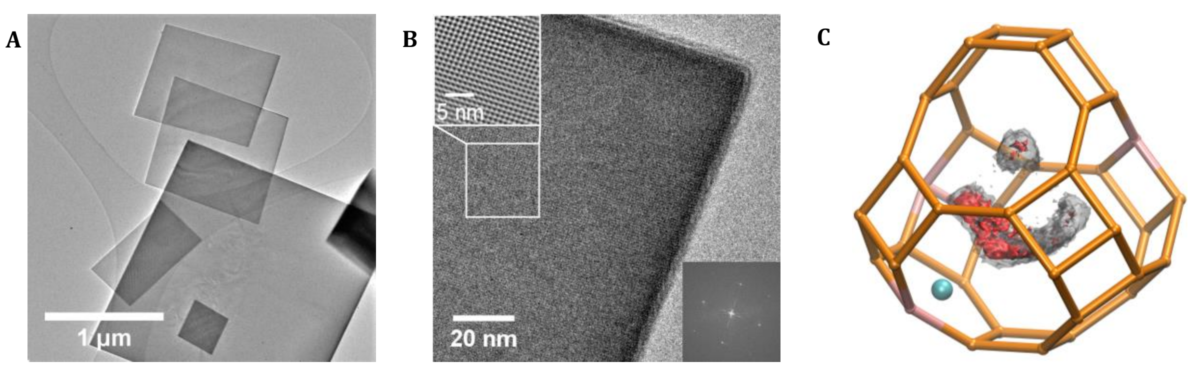

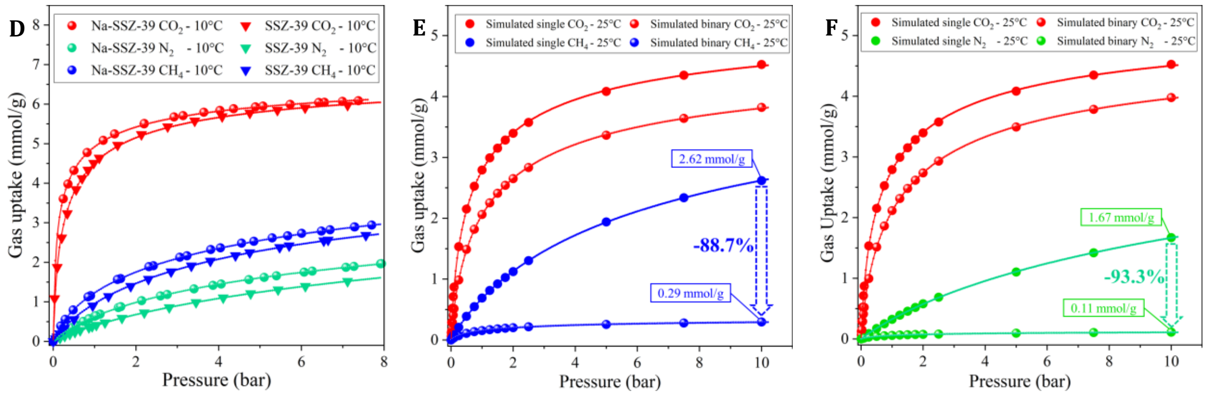

Fig. 1. SSZ-39 zeolite. (**A**). TEM image of Na-SSZ-39 platelet, and (**B**) of its base-face, the top-left shows a Fourier-filtered image from the selected area, and the bottom-right presents the Fourier-transform of this image, thus proving the base-face refers to the [0 0 1] crystal plane of the AEI-type framework (Fig. S47); (**C**) 3D density iso-surface for CO_2 adsorption in a Na-SSZ-39 cage at 0.1 bar (in red) and 1 bar (in gray) under 25 °C (by GCMC, where (3×1/3) Al-sites are pink, Na^+ is cyan, O is omitted), indicating that the Na^+ is a preferential adsorption site particularly at lower pressures. At higher pressures, additional molecules are adsorbed, occupying the remaining space of the cage. (**D**) Experimental CO_2, CH_4 and N_2 adsorption isotherms of SZZ-39 and Na-SSZ-39 zeolites at 10 ºC; (**E**) single-gas and equimolar mixed-gas CO_2/CH_4 adsorption isotherms of Na-SSZ-39 zeolite at 25 °C (by GCMC); (**F**) single-gas and equimolar mixed-gas CO_2/N_2 adsorption isotherms of Na-SSZ-39 zeolite at 25 °C (by GCMC). (details in SI)

MMM characterization

Self-standing MMMs were prepared with Na-SSZ-39 reaching extremely high loadings up to 55 wt.% (Fig. 4B). XRD confirmed the preservation of zeolite crystallinity in MMMs after all synthesis steps (Fig. S13). SEM membrane cross-sections (Fig. 2A) show that the zeolite platelets are positioned in the polymer matrix in a random, non-aligned packing. This homogeneous distribution of zeolite platelets at high loading was realized through a subtle and carefully optimized interplay between zeolite and casting solution during MMM synthesis. More specifically, favorable molecular interactions between zeolite and the Matrimid/chloroform solution were combined with a small density difference between zeolite and solvent (~1.55 g/cm^3 and ~1.49 g/cm^3 respectively), the high-aspect-ratio of the filler, a high viscosity of the casting solution, dedicated evaporation control of the solvent and thermal annealing. After membrane solidification, remaining interfacial defects were eliminated by a tuned annealing protocol, which had a profound impact on the final MMM performance (Fig. S59). The 180 ºC annealing program resulted in slightly more permeable membranes than the 260 ºC program, but the 260 ºC program induced a far higher CO_2/CH_4 selectivity (for 50 wt.% Na-SSZ-39 MMM, the selectivity increased from ~200 to >420; Table S5), while the 350 ºC program resulted in fragile and brittle carbonized membranes. Fig. 2C shows that 260 ºC-annealed membranes did not show sieve-in-a-cage morphology, which traditionally is a major issue for zeolite MMMs (*31*). Compared to its non-annealed counterparts (Fig. 2B), a much better zeolite-polymer adhesion can be observed (Fig. S54-S55). Full removal of the polymer by oxidative treatment at 800 °C (Fig. S51) led to a stable zeolite-only film (Fig. 2D-2E, Fig. S51-S53), confirming the high zeolite loading in a random packing. This nearly-continuous zeolite phase across the MMM thus creates a ‘percolation highway’ to allow ultrafast permeation of the selected gas molecules.

As anticipated, both FT-IR and Raman microspectroscopy could not find evidence for a covalent interaction between polymer and zeolite after annealing (Fig. S18 and S61-S66). DSC analysis indicated very good polymer-zeolite interactions in the MMM: with the Na-SSZ-39 loading, the glass transition temperature increased from 314 ºC (for Matrimid) to 325 ºC (for annealed Na-SSZ-39 MMMs), pointing towards ‘wrapping’ of the zeolite by polymer and rigidification of the polymer chains at the interface (Fig. S17). CO_2, CH_4 and N_2 sorption experiments were performed on the 260 ºC annealed Matrimid membrane and the 50 wt.% Na-SSZ-39 MMM to quantify their respective gas uptake. A substantially higher gas uptake was denoted for the MMM (Fig. S30).

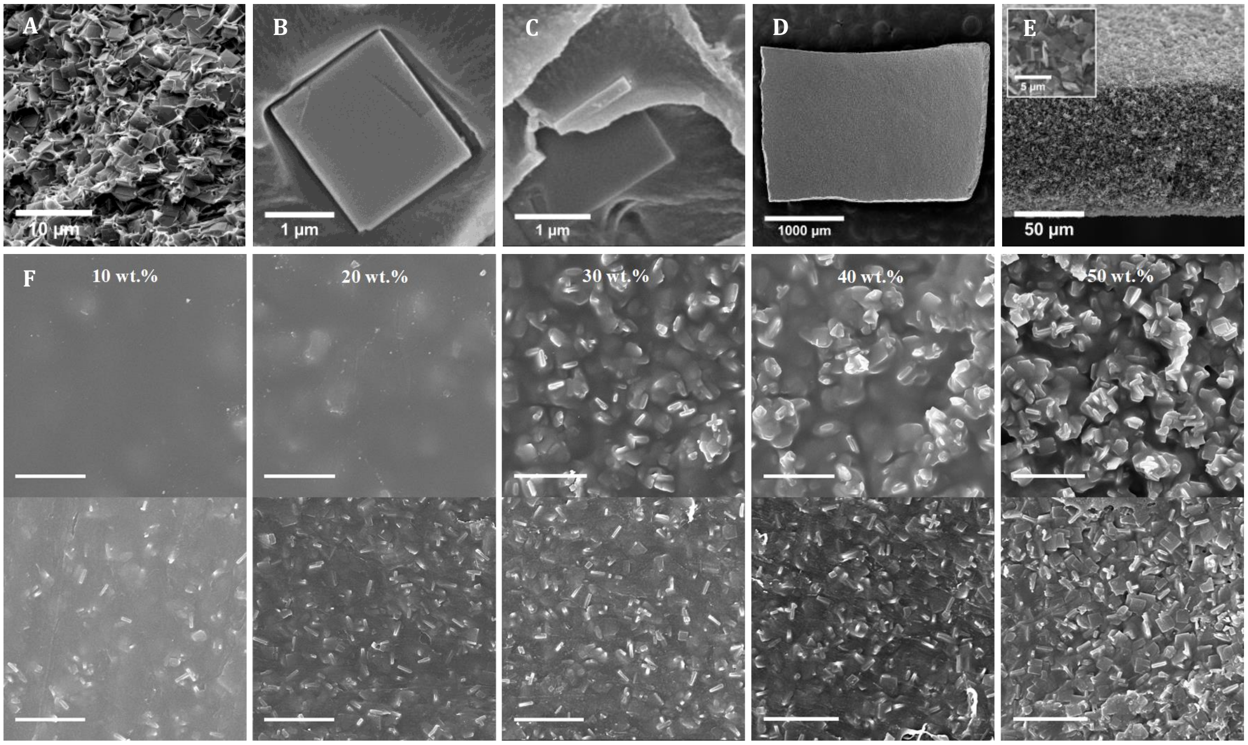

Fig. 2. SEM images of the platelet-shaped Na-SSZ-39 MMMs. (**A**). cross-section of the 40 wt.% Na-SSZ-39 MMM after 260 ºC annealing; (**B**). cross-section of 20 wt.% Na-SSZ-39 MMM before and (**C**) after annealing; (**D**, **E**). top-view and cross-section of the 30 wt.% Na-SSZ-39 MMM after 800 °C oxidative treatment, burning off the polymer (Fig. S51-S53); (**F**). top-view (above) and bottom-view (below) of membranes with 10-50 wt.% platelet-shaped zeolite loading (scale bar =10 µm in **F**). (details in SI)

Membrane gas separation performance

The mixed-gas selectivities of Na-SSZ-39 MMMs (Table S5) were significantly higher than their ideal-gas selectivities (Table S8), due to the competitive sorption of CO_2 in the Na-SSZ-39 zeolite. For instance, for the 50 wt.% Na-SSZ-39 MMM, the CO_2/CH_4 ideal gas selectivity was ~336 (1 bar/25 ºC), while the equimolar CO_2/CH_4 mixed-gas selectivity reached >420 (2 bar/25 ºC, i.e. 1 bar CO_2 and CH_4 partial pressures). Likewise, the CO_2/N_2 ideal-gas selectivity at 1 bar/25 ºC was ~32, while its mixed gas selectivity at 2 bar/25 ºC increased to ~60. Once the stronger adsorbing CO_2 occupied the adsorption sites, the zeolite channels become partly inaccessible for the other gas, thus inhibiting permeation of CH_4 and N_2.

Based on the physisorption and ideal-gas permeation results, gas solubility/diffusivity values were calculated for the unfilled Matrimid membrane and 50 wt.% Na-SSZ-39 MMM (Table S20). With respect to the unfilled membrane, the MMM displayed a 4.6 times higher CO_2 solubility whereas the CH_4 and N_2 solubility increased 7.5 and 3.4 times, respectively. A 220-fold increase in CO_2 diffusivity was denoted for the MMM compared to the unfilled Matrimid membrane, while CH_4 and N_2 diffusivity only increased 14 and 148 times, respectively. The enhancement of CO_2/CH_4 diffusivity selectivity thus explains the strong improvement of the MMM gas separation capability (Table S21). This results from the sharp size-sieving effect of Na-SSZ-39 for the CO_2/CH_4 pair. The increase in diffusivity selectivity for CO_2/N_2 is less pronounced as N_2 possesses a smaller kinetic diameter. The notable difference in separation factor for CO_2/CH_4 and CO_2/N_2 confirms the central role of the highly accurate size-sieving mechanism for the stunning selectivities of Na-SSZ-39 MMMs.

Mixed-gas CO_2/CH_4 and CO_2/N_2 separation performances are presented in Fig. 3. For CO_2/CH_4, a continuous increase in separation factor is observed with increasing Na-SSZ-39 loading. Whereas the unfilled Matrimid membrane denotes a CO_2/CH_4 separation factor of ~45 and CO_2 permeability ~8 Barrer, the best MMM performance was obtained with the 50 wt.% Na-SSZ-39 loading, which obtained a selectivity of >420 at 2 bar/25 °C (~10-fold increase), at a simultaneous extreme CO_2 permeability of ~8280 Barrer (~1037-fold increase). Similar results were obtained for the CO_2/N_2 separation performance where the 50 wt.% MMM combined a CO_2 permeability of >8300 Barrer with a CO_2/N_2 separation factor of ~60 (vs ~8 and ~35 for unfilled Matrimid). Fig. 3B–3C show the temperature and pressure dependency of the membrane performance with different zeolite loadings. With increasing temperature, the CO_2 adsorption in the zeolite obviously decreased (Fig. S27), resulting in lowered CO_2 permeability and CO_2/CH_4 selectivity. Similar behavior was observed with rising feed pressure: both CO_2 permeability and CO_2/CH_4 selectivity reduced. Because of its high CO_2-philicity, Na-SSZ-39 is already saturated with CO_2 molecules at low feed pressure. Further increased pressures thus contribute less to CO_2 permeation. For the same reason, the Na-SSZ-39 MMMs exhibit enhanced performance in feeds with lower CO_2 partial pressures (Table S6). For instance, the 50 wt.% Na-SSZ-39 MMM gave a CO_2 permeability of >10000 Barrer and a CO_2/CH_4 selectivity >460 for a 20 vol.% CO_2/80 vol.% CH_4 feed (Fig. S23-S24), which is close to the compositions of industrial feed streams, such as certain bio-gas and natural gas sources (*39*, *40*).

When depicted on selectivity-permeability trade-off plots, the Na-SSZ-39 MMMs already surpass the 2008 Robeson upper-bound (*11*) from 30 wt.% loading onward for CO_2/N_2 (Fig. 3D) and even from 20 wt.% for CO_2/CH_4 (Fig. 3E). Ultimately, they realize an unprecedented jump towards the upper-right corner of the Robeson plot, ending up even beyond the performance area that is dominated by zeolite-only membranes (Fig. 3F). Outperforming the existing zeolite-only membranes can be related to the properties of the Na-SSZ-39 filler as well as the membrane morphology. Moreover, compared to the zeolite-only membranes, the Na-SSZ-39 MMMs additionally keep their flexibility because of the presence of the polymer matrix (Fig. 4A, Movie S2). Furthermore, due to the exceptional stability of the Na-SSZ-39 filler and the thermal annealing protocol, the Na-SSZ-39 MMMs possess anti-ageing properties. Although the ageing characteristics may vary with film thickness, the self-standing 50 wt.% Na-SSZ-39 MMM shows comparable CO_2/CH_4 selectivity and CO_2 permeability even 360 days after preparation (Table S5). From an application point of view in the frame of CO_2-removal, this anti-ageing, high-flux and high-selectivity membrane can allow significant reductions in both operational and capital costs, as a simplified and more energy-efficient operation scheme with less recycling and milder (re-)compression stages can be applied, in combination with reduced membrane areas and less replacement (*2*–*3*).

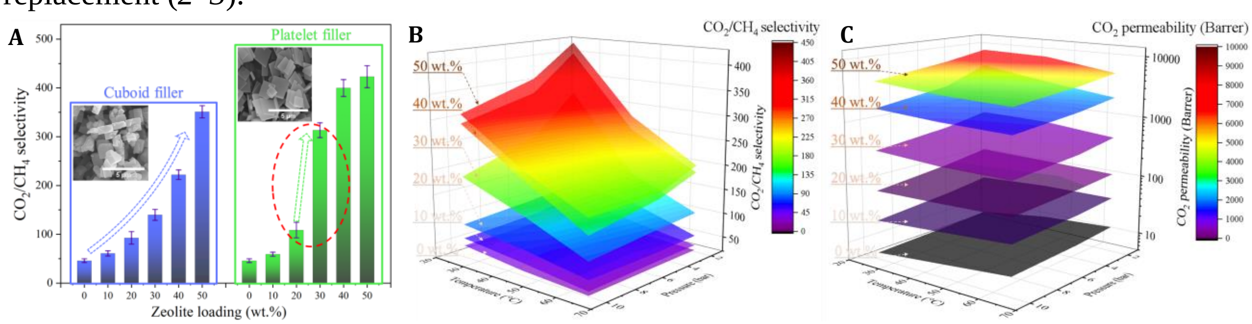

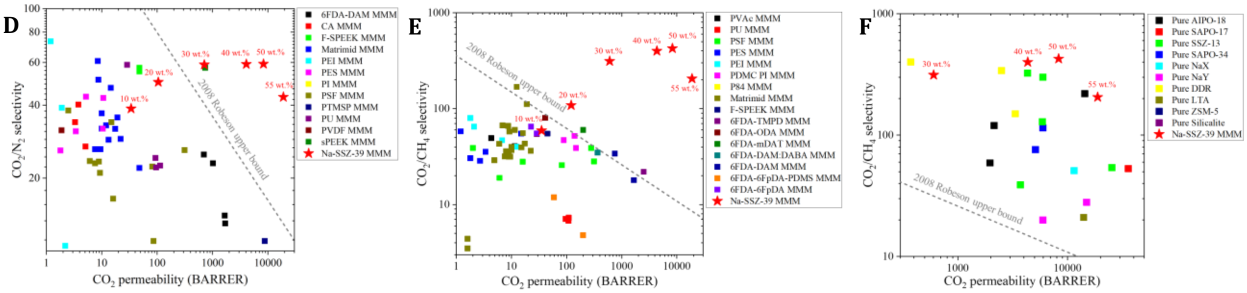

Fig. 3. The gas separation performances of Na-SSZ-39 MMMs. (**A**). the selectivity difference between cuboid-shaped and platelet-shaped Na-SSZ-39 MMMs, the inset SEM images show the morphology difference of two zeolites; (**B, C**). the temperature and pressure dependence of CO_2/CH_4 selectivity and CO_2 permeability (9-points constitute a plane); (**D**, **E**). the performance of zeolite-filled MMMs from literature are shown in CO_2/N_2 and CO_2/CH_4 2008 Robeson plots; the red stars represent the platelet-shaped Na-SSZ-39 MMMs; (**F**). the pure zeolite membranes from literature compared with the Na-SSZ-39 MMMs (≥30 wt.%) and 2008 CO_2/CH_4 Robeson plot (full datasets available in SI).

The gas separation performance of the Na-SSZ-39 MMMs can thus be explained by a combination of three factors.

First, the selection of the Na-SSZ-39 zeolite as membrane filler is critical. Due to its accurate molecular size-sieving effect and strong CO_2-philicity, Na-SSZ-39 possesses enormous diffusivity and solubility selectivities, thus promoting ultra-high mixed-gas selectivity. Moreover, the non-centrosymmetric AEI-type framework allows preparation of high-aspect-ratio platelets. In contrast to many high-aspect-ratio porous materials that possess 1D-channels perpendicular to their base-face (*41–42*), the SSZ-39 platelet is equipped with a 3D-channel system with 3.84 Å windows in its lateral face (Fig. 1B). Therefore, regardless of the platelet's orientation inside the membrane, the SSZ-39 pore system always allows unhindered gas flow (Fig. 4D–4E).

Second, the sudden jump in CO_2/CH_4 separation factor at 20-30 wt.% loading suggests a percolation effect (Fig. 3A), i.e. from this loading onward, gas permeation through the membrane is predominantly going through the zeolite phase. The reason for this shift in phase dominance should be sought in the practical ability to incorporate ultra-high loadings of the high-aspect-ratio filler in the polymer. This creates a membrane morphology, which consists of a quasi-continuous zeolite phase across the membrane starting from only 20-30 wt.% loading (Fig. 4D) and allows for percolation of the gas molecules with minimal influence of the less permeable polymer phase. The top and bottom views (Fig. 2F) of the MMMs show that the zeolite platelets pile up from the bottom and appear at the top of membrane when the zeolite loading reaches 30 wt.% (Fig. 4C). In this context, the non-aligned, randomly-oriented Na-SSZ-39 platelet distribution which leads to a selective gas permeation highway, is a key driver and prerequisite for the membrane's extraordinary performance. This was also confirmed by comparing the platelet-shaped Na-SSZ-39 filler with a cuboid-shaped one (with similar properties except the aspect-ratio, as per SI). As Fig. 3A shows, the sudden increment in CO_2/CH_4 selectivity was only observed for the platelet-shaped Na-SSZ-39 MMMs. Furthermore, although the cuboid-shaped Na-SSZ-39 MMMs also show great performances, the platelet-shaped Na-SSZ-39 MMMs exhibited far better CO_2/CH_4 selectivity and CO_2 permeability (Table S5-S13), thus further confirming the morphology benefits of platelet-shaped Na-SSZ-39 MMMs.

Finally, as the overall gas transport through the MMM is a net result of the properties of both zeolite and polymer, as well as of their mutual interactions, it is crucial to obtain a defect-free zeolite/polymer interface. Although rubbery polymers, like PDMS, facilitate creation of a defect-free interface (Fig. S60), their intrinsically low selectivity and high permeability neutralize the beneficial contribution of the zeolite (Table S15). The well-designed membrane preparation strategy minimizes the occurrence of unselective voids at the zeolite-Matrimid interface (Fig. S54-55, S58-59), allowing for ultra-high zeolite loadings of >50 wt.% without chemical modification of zeolite or polymer, nor use of additives. Even at these high loadings, the Na-SSZ-39 MMMs still maintain desired flexibility (Fig. 4A), thus also creating excellent opportunities for module construction and upscaling.

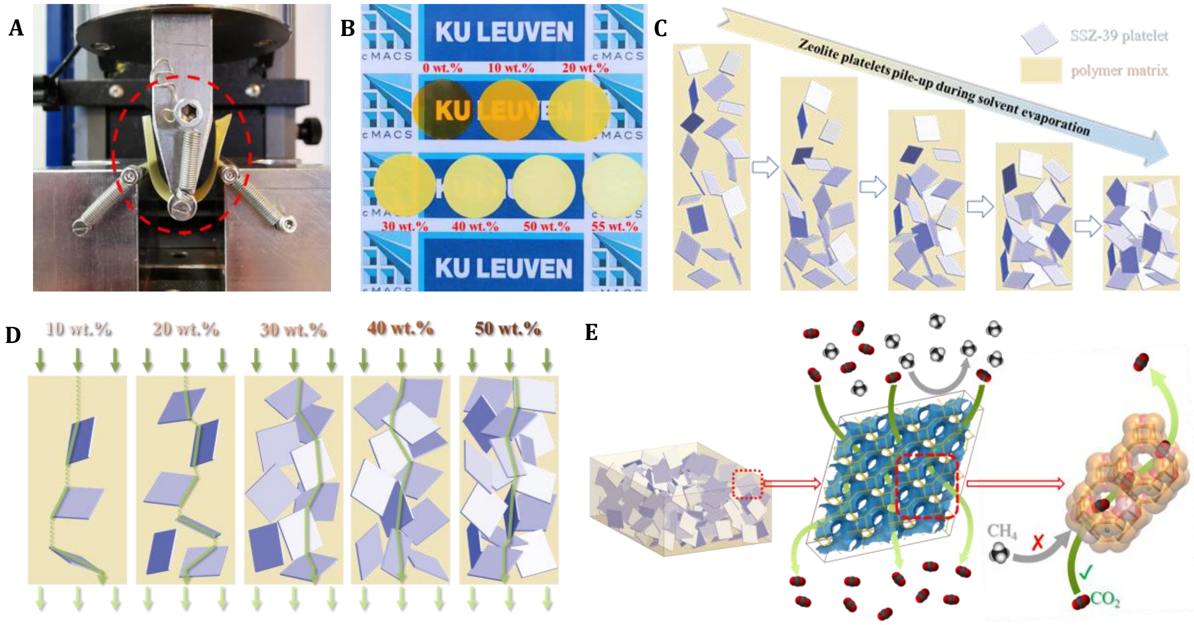

Fig. 4. Characterization and illustrations of platelet-shaped Na-SSZ-39 MMM. (**A**) the flexibility test (3-points bending) for 50 wt.% Na-SSZ-39 MMM (Table S4); (**B**) visual appearance of 0-55 wt.% Na-SSZ-39 MMMs; (**C**) illustration of the solidification process of the platelet-shaped Na-SSZ-13 MMM, resulting in a quasi-continuous zeolite phase across the membrane; (**D**) illustration of the non-aligned zeolite platelet distribution in the polymer matrix with different zeolite loading, the preferential gas permeation pathways are indicated by the green arrows; (**E**) schematic illustration of a MMM with quasi-continuous zeolite phase (left-picture) and the unhindered CO_2 permeation (represented by the green arrows) through the 3D-channel system of platelet-shaped Na-SSZ-39 filler regardless of its orientation (middle-picture), as well as the precise molecular sieving behavior which excludes CH_4 from CO_2 via the zeolite window (right-picture).

Conclusions

An ultra-high-performance zeolite-filled MMM for CO_2 separations was developed, showing unprecedented CO_2 removal performance, not only higher than any existing polymeric membrane or MMM, but even surpassing most zeolite-only membranes. By circumventing the traditional incompatibility between zeolite filler and glassy polymer matrix, a flexible, defect-free zeolite/polyimide MMM with ultra-high (>50 wt.%) zeolite loadings were prepared. Na-SSZ-39 zeolite was discovered as a superior filler, due to its outstanding CO_2-philicity, precise molecular-sieving windows, strong competitive sorption behavior and excellent stability, promoting stunning, non-ageing CO_2 separation performances. Due to the high-aspect-ratio and 3D-channel system of the filler, a percolating gas permeation highway was created across the membrane, thus drastically enhancing the membrane's performance.

A scalable method was used to prepare defect-free zeolite-filled membranes with a commercially-available glassy polymer, thus opening the door to developing well-processable, robust and economical high-performance zeolite-filled MMM for a variety of gas and liquid separations. It is especially beneficial for those zeolites that are difficult to be engineered into defect-free zeolite-only films.

References and Notes

1. D.S. Sholl, R. P. Lively, Seven chemical separations. *Nature*. **532**, 435–437 (2016). doi:10.1038/532435a
2. R. W. Baker, *Membrane Technology and Applications* (JohnWiley & Sons, Inc., ed. 3, Hoboken, NJ, 2012).
3. S. P. Nunes, K.-V. Peinemann, *Membrane Technology: in the Chemical Industry* (Wiley-VCH, ed. 2, Weinheim, Germany, 2006).
4. P. Bernardo, E. Drioli, G. Golemme, Membrane gas separation: A review/state of the art. *Ind. Eng. Chem. Res.* **48**, 4638–4663 (2009). doi:10.1021/ie8019032
5. R. W. Baker, B. T. Low, Gas separation membrane materials: A perspective. *Macromolecules*. **47**, 6999–7013 (2014). doi:10.1021/ma501488s
6. C. A. Scholes, G. W. Stevens, S. E. Kentish, Membrane gas separation applications in natural gas processing. *Fuel*. **96**, 15–28 (2012). doi:10.1016/j.fuel.2011.12.074
7. S. Basu, A. L. Khan, A. Cano-Odena, C. Liu, I. F. J. Vankelecom, Membrane-based technologies for biogas separations. *Chem. Soc. Rev.* **39**, 750–768 (2010). doi:10.1039/b817050a
8. S. K. Simons, K. Nijmeijer, M. Wessling, Gas–liquid membrane contactors for CO2 removal, *J. Membr. Sci.* **340**, 214–220 (2009). doi:org/10.1016/j.memsci.2009.05.035
9. G. He, S. Huang, L. F. Villalobos, J. Zhao, M. Mensi, E. Oveisi, M. Rezaei, K. V. Agrawal, High-permeance polymer-functionalized single-layer graphene membranes that surpass the postcombustion carbon capture target. *Energy Environ. Sci.* **12**, 3305–3312 (2019). doi:10.1039/C9EE01238A
10. M. E. Boot-Handford, J. C. Abanades, E. J. Anthony, M. J. Blunt, S. Brandani, N. Mac Dowell, J. R. Fernández, M. C. Ferrari, R. Gross, J. P. Hallett, R. S. Haszeldine, P. Heptonstall, A. Lyngfelt, Z. Makuch, E. Mangano, R. T. J. Porter, M. Pourkashanian, G. T. Rochelle, N. Shah, J. G. Yao, P. S. Fennell, Carbon capture and storage update. *Energy Environ. Sci.* **7**, 130–189 (2014). doi:10.1039/C3EE42350F
11. L. M. Robeson, The upper bound revisited. *J. Memb. Sci.* **320**, 390–400 (2008). doi:10.1016/j.memsci.2008.04.030
12. H. B. Park, J. Kamcev, L. M. Robeson, M. Elimelech, B. D. Freeman, Maximizing the right stuff: The trade-off between membrane permeability and selectivity. *Science* **356**, 1138–1148 (2017). doi:10.1126/science.aab0530
13. B. Comesaña-Gándara, J. Chen, C. G. Bezzu, M. Carta, I. Rose, M. C. Ferrari, E. Esposito, A. Fuoco, J. C. Jansen, N. B. McKeown, Redefining the Robeson upper bounds for CO2/CH4 and CO2/N2 separations using a series of ultrapermeable benzotriptycene-based polymers of intrinsic microporosity. *Energy Environ. Sci.* **12**, 2733–2740 (2019). doi:10.1039/C9EE01384A
14. N. Du, H. B. Park, G. P. Robertson, M. M. Dal-Cin, T. Visser, L. Scoles, M. D. Guiver,

Polymer nanosieve membranes for CO2-capture applications. *Nat. Mater.* **10**, 372–375 (2011). doi:10.1038/nmat2989

15. M. Carta, R. Malpass-Evans, M. Croad, Y. Rogan, J. C. Jansen, P. Bernardo, F. Bazzarelli, N. B. McKeown, An efficient polymer molecular sieve for membrane gas separations. *Science* **339**, 303–307 (2013). doi:10.1126/science.1228032
16. H. W. H. Lai, F. M. Benedetti, J. M. Ahn, A. M. Robinson, Y. Wang, I. Pinnau, Z. P. Smith, Y. Xia, Hydrocarbon ladder polymers with ultrahigh permselectivity for membrane gas separations. *Science*. **375**, 1390-1392 (2022). doi:10.1126/science.abl7163
17. Z. Lai, G. Bonilla, I. Diaz, J. G. Nery, K. Sujaoti, M. A. Amat, E. Kokkoli, O. Terasaki, R. W. Thompson, M. Tsapatsis, D. G. Vlachos, Microstructural Optimization of a Zeolite Membrane for Organic Vapor Separation. *Science* **300**, 456–460 (2003). doi:10.1126/science.1082169
18. N. Rangnekar, N. Mittal, B. Elyassi, J. Caro, M. Tsapatsis, Zeolite membranes - a review and comparison with MOFs. *Chem. Soc. Rev.* **44**, 7128–7154 (2015). doi:10.1039/C5CS00292C
19. M. Y. Jeon, D. Kim, P. Kumar, P. S. Lee, N. Rangnekar, P. Bai, M. Shete, B. Elyassi, H. S. Lee, K. Narasimharao, S. N. Basahel, S. Al-Thabaiti, W. Xu, H. J. Cho, E. O. Fetisov, R. Thyagarajan, R. F. Dejaco, W. Fan, K. A. Mkhoyan, J. I. Siepmann, M. Tsapatsis, Ultra-selective high-flux membranes from directly synthesized zeolite nanosheets. *Nature*. **543**, 690–694 (2017). doi:10.1038/nature21421
20. X. Ma, P. Kumar, N. Mittal, A. Khlyustova, P. Daoutidis, K. Andre Mkhoyan, M. Tsapatsis, Zeolitic imidazolate framework membranes made by ligand-induced permselectivation. *Science* **361**, 1008–1011 (2018). doi:10.1126/science.aat4123
21. N. Kosinov, J. Gascon, F. Kapteijn, E. J. M. Hensen, Recent developments in zeolite membranes for gas separation. *J. Memb. Sci.* **499**, 65–79 (2016). doi:10.1016/j.memsci.2015.10.049
22. W. J. Koros, C. Zhang, Materials for next-generation molecularly selective synthetic membranes. *Nat. Mater.* **16**, 289–297 (2017). doi:10.1038/nmat4805
23. S. Wang, X. Li, H. Wu, Z. Tian, Q. Xin, G. He, D. Peng, S. Chen, Y. Yin, Z. Jiang, M. D. Guiver, Advances in high permeability polymer-based membrane materials for CO2 separations. *Energy Environ. Sci.* **9**, 1863–1890 (2016). doi:10.1039/C6EE00811A
24. J. E. Bachman, Z. P. Smith, T. Li, T. Xu, J. R. Long, Enhanced ethylene separation and plasticization resistance in polymer membranes incorporating metal-organic framework nanocrystals. *Nat. Mater.* **15**, 845–849 (2016). doi:10.1038/nmat4621
25. A. Kertik, L. H. Wee, M. Pfannmöller, S. Bals, J. A. Martens, I. F. J. Vankelecom, Highly selective gas separation membrane using in-situ amorphised metal-organic frameworks. *Energy Environ. Sci.* **10**, 2342–2351 (2017). doi:10.1039/C7EE01872J
26. B. Wang, Z. Qiao, J. Xu, J. Wang, X. Liu, S. Zhao, Z. Wang, M. D. Guiver, Unobstructed Ultrathin Gas Transport Channels in Composite Membranes by Interfacial Self-Assembly. *Adv. Mater.* **32,** 1907701 (2020). doi:10.1002/adma.201907701
27. B. Seoane, J. Coronas, I. Gascon, M. E. Benavides, O. Karvan, J. Caro, F. Kapteijnaand, J. Gascon, Metal–organic framework based mixed matrix membranes: a solution for highly

efficient CO2 capture?. *Chem. Soc. Rev.* **44,** 2421-2454 (2015). doi:org/10.1039/C4CS00437J

28. J. Dechnik, J. Gascon, C. J. Doonan, C. Janiak, C. J. Sumby, Mixed-Matrix Membranes. *Angew. Chemie - Int. Ed.* **56**, 9292–9310 (2017). doi:10.1002/anie.201701109
29. M. Galizia, W. S. Chi, Z. P. Smith, T. C. Merkel, R. W. Baker, B. D. Freeman, 50th Anniversary Perspective: Polymers and Mixed Matrix Membranes for Gas and Vapor Separation: A Review and Prospective Opportunities. *Macromolecules*. **50**, 7809–7843 (2017). doi:10.1021/acs.macromol.7b01718
30. I. F. Vankelecom, E.Scheppers, R. Heus, J. B. Uytterhoeven. Parameters influencing zeolite incorporation in PDMS membranes. *J. Phys. Chem.* **98**, 12390-12396 (1994). doi:10.1021/j100098a038
31. R. Mahajan, R. Burns, M. Schaeffer, W. J. Koros, Challenges in forming successful mixed matrix membranes with rigid polymeric materials. *J. Appl. Polym. Sci.* **86**, 881–890 (2002). doi:10.1002/app.10998
32. D. Bastani, N. Esmaeili, M. Asadollahi, Polymeric mixed matrix membranes containing zeolites as a filler for gas separation applications: A review. *J. Ind. Eng. Chem.* **19**, 375–393 (2013). doi:10.1016/j.jiec.2012.09.019
33. S. I. Zones, Y. Nakagawa, S. T. Evans, G. S. Lee, US 5,958,370A, (1999).
34. N. Nakazawa, S. Inagaki, Y. Kubota, Direct Hydrothermal Synthesis of High-silica SSZ-39 Zeolite with Small Particle Size. *Chem. Lett.* **45**, 919–921 (2016). doi:10.1246/cl.160370
35. M. Dusselier, J. E. Schmidt, R. Moulton, B. Haymore, M. Hellums, M. E. Davis, Influence of organic structure directing agent isomer distribution on the synthesis of SSZ-39. *Chem. Mater.* **27**, 2695–2702 (2015). doi:10.1021/acs.chemmater.5b00651
36. M. Dusselier, M. E. Davis, Small-Pore Zeolites: Synthesis and Catalysis. *Chem. Rev.* **118**, 5265–5329 (2018). doi:10.1021/acs.chemrev.7b00738
37. Ch. Baerlocher, L. B. McCusker, Database of Zeolite Structures(2017); http://www.iza-structure.org/databases.
38. T. D. Pham, Q. Liu, R. F. Lobo, Carbon dioxide and nitrogen adsorption on cation-exchanged SSZ-13 zeolites. *Langmuir*. **29**, 832–839 (2013). doi:10.1021/la304138z
39. S. Faramawy, T. Zaki, A. A. E. Sakr, Natural gas origin, composition, and processing: A review. *J. Nat. Gas Sci. Eng.* **34**, 34–54 (2016). doi:10.1016/j.jngse.2016.06.030
40. Y. Li, C. P. Alaimo, M. Kim, N. Y. Kado, J. Peppers, J. Xue, C. Wan, P. G. Green, R. Zhang, B. M. Jenkins, C. F. A. Vogel, S. Wuertz, T. M. Young, M. J. Kleeman, Composition and Toxicity of Biogas Produced from Different Feedstocks in California. *Environ. Sci. Technol.* **53,** 11569–11579 (2019). doi:10.1021/acs.est.9b03003
41. T. Rodenas, I. Luz, G. Prieto, B. Seoane, H. Miro, A. Corma, F. Kapteijn, F. X. Llabrés I Xamena, J. Gascon, Metal-organic framework nanosheets in polymer composite materials for gas separation. *Nat. Mater.* **14**, 48–55 (2015). doi:10.1038/nmat4113
42. S. J. Datta, A. Mayoral, N. M. S. Bettahalli, P. M. Bhatt, M. Karunakaran, I. D. Carja, D. Fan, P. G. M. Mileo, R. Semino, G. Maurin, O. Terasaki, M. Eddaoudi, Rational design of mixed-matrix metal-organic framework membranes for molecular separations. *Science*

1087, 1080–1087 (2022). doi:10.1126/science.abe0192

43. Y. Cheng, Z. Wang, D. Zhao, Mixed Matrix Membranes for Natural Gas Upgrading: Current Status and Opportunities. *Ind. Eng. Chem. Res.* **57**, 4139–4169 (2018). doi:10.1021/acs.iecr.7b04796

44. R. W. Baker, K. Lokhandwala, Natural gas processing with membranes: An overview. *Ind. Eng. Chem. Res.* **47**, 2109–2121 (2008). doi:10.1021/ie071083w

45. B. D. Freeman, Basis of perme ability/selectivity trade off relations in polymeric gas separation membranes. *Macromolecules* **32**, 375–380 (1999). doi:10.1021/ma9814548

46. M. Tsapatsis, Toward High-Throughput Zeolite Membranes. *Science* **334**, 767-768 (2011). doi:10.1126/science.1205957

47. M. Sandru, E. M. Sandru, P. M. Stenstad, W. F. Ingram, J. Deng, An Integrated Materials Approach to Ultrapermeable and Ultraselective CO2 Polymer Membranes: Breaking through the Upper Bound. *Science* **94**, 90–94 (2022). doi:10.1126/science.abj9351

48. S. Yi, B. Ghanem, Y. Liu, I. Pinnau, W. J. Koros, Ultraselective glassy polymer membranes with unprecedented performance for energy-efficient sour gas separation. *Sci. Adv.* **5**, 1–12 (2019). doi:10.1126/sciadv.aaw5459

49. H. W. Kim, H. W. Yoon, S.-M. Yoon, B. M. Yoo, B. K. Ahn, Y. H. Cho, H. J. Shin, H. Yang, U. Paik, S. Kwon, J.-Y. Choi, H. B. Park, Selective gas transport through few-layered graphene and graphene oxide membranes. *Science* **342**, 91–95 (2013). doi:10.1126/science.1236098

50. H. Li, Z. Song, X. Zhang, Y. Huang, S. Li, Y. Mao, H. J. Ploehn, Y. Bao, M. Yu, Ultrathin, molecular-sieving graphene oxide membranes for selective hydrogen separation. *Science.* **342**, 95–98 (2013). doi:10.1126/science.1236686

51. J. Liu, S. Zhang, D. en Jiang, C. M. Doherty, A. J. Hill, C. Cheng, H. B. Park, H. Lin, Highly Polar but Amorphous Polymers with Robust Membrane CO2/N2 Separation Performance. *Joule*. **3**, 1881–1894 (2019). doi:10.1016/j.joule.2019.07.003

52. J. H. Kang, F. H. Alshafei, S. I. Zones, M.E. Davis, Cage-Defining Ring: A molecular Sieve Structural Indicator for Light Olefin Product Distribution from the Methanol-to-Olefins Reaction. *ACS Catal.* **9**, 6012−6019 (2019). doi:10.1021/acscatal.9b00746

53. A. L. Khan, S. Basu, A. Cano-Odena, I. F. Vankelecom, Novel high throughput equipment for membrane-based gas separations. *J. Membr. Sci.* **354**, 32-39 (2010). doi:10.1016/j.memsci.2010.02.069

54. J. Didden, R. Thur, A. Volodin, I. F. Vankelecom, Blending PPO-Based Molecules with Pebax MH 1657 in Membranes for Gas Separation. *J. Appl. Polym. Sci.* **135**, 46433 (2018). doi:10.1002/app.46433

55. M. Klinger, A. Jäger, Crystallographic Tool Box (CrysTBox): automated tools for transmission electron microscopists and crystallographers. *J. Appl. Cryst.* **48**, 2012-2018 (2015). doi:10.1107/S1600576715017252

56. J. Tóth, State equation of the solid-gas interface layers. *Acta Chem. Acad. Sci. Hung.* **69**, 311–328 (1971).

57. D. D. Duong, *Adsorption Analysis: Equilibria and Kinetics.* (Series on Chemical

Engineering, World Scientific, 1998), Vol 2. doi:10.1142/p111

58. A.L. Myers, J.M. Prausnitz, Thermodynamics of mixed-gas adsorption. *AIChE J.* **11**, 121-127 (1965) doi:10.1002/aic.690110125

59. K.S. Walton, D.S. Sholl, Prediciting Multicomponent Adsorption: 50 Years of the Ideal Adsorbed Solution Theory. *AIChE J.* **61**, 2757-2762 (2015). doi:10.1002/aic.14878

60. D. Dubbeldam, S. Calero, D. E. Ellis, R. Q. Snurr, RASPA: molecular simulation software for adsorption and diffusion in flexible nanoporous materials. *Mol. Simulat.* **42**, 81–101 (2016). doi:10.1080/08927022.2015.1010082

61. E. García-Pérez, J. B. Parra, C. O. Ania, A. García-Sánchez, J. M. van Baten, R. Krishna, D. Dubbeldam, and S. Calero, A computational study of CO2, N2, and CH4 adsorption in zeolites. *Adsorption.* **13**, 469–476 (2007). doi:10.1007/s10450-007-9039-z

62. A. Martin-Calvo, J. J. Gutiérrez-Sevillano, J. B. Parra, C. O. Ania, S. Calero, Transferable force fields for adsorption of small gases in zeolites. *Phys. Chem. Chem. Phys.* **17**, 24048–24055 (2015). doi:10.1039/c5cp03749b

63. T. D. Kühne, M. Iannuzzi, M. Del Ben, V. V. Rybkin, P. Seewald, F. Stein, T. Laino, R. Z. Khaliullin, O. Schütt, F. Schiffmann, D. Golze, J. Wilhelm, S. Chulkov, M. H. Bani-Hashemian, V. Weber, U. Borštnik, M. Taillefumier, A. S. Jakobovits, A. Lazzaro, H. Pabst, T. Müller, R. Schade, M. Guidon, S. Andermatt, N. Holmberg, G. K. Schenter, A. Hehn, A. Bussy, F. Belleflamme, G. Tabacchi, A. Glöß, M. Lass, I. Bethune, C. J. Mundy, C. Plessl, M. Watkins, J. VandeVondele, M. Krack, J. Hutter, CP2K: An electronic structure and molecular dynamics software package - Quickstep: Efficient and accurate electronic structure calculations. *J. Chem. Phys.* **152**, 194103 (2020). doi:10.1063/5.0007045

64. S. Nosé, A molecular dynamics method for simulations in the canonical ensemble. *Mol. Phys.* **52**, 255–268 (1984). doi:10.1080/00268978400101201

65. S. Nosé, A unified formulation of the constant temperature molecular dynamics methods. *J. Chem. Phys.* **81**, 511–519 (1984). doi:10.1063/1.447334

66. G. J. Martyna, D. J. Tobias, M. L. Klein, Constant pressure molecular dynamics algorithms. *J. Chem. Phys.* **101**, 4177–4189 (1994). doi:10.1063/1.467468

67. J. P. Perdew, K. Burke, M. Ernzerhof, Generalized Gradient Approximation Made Simple. *Phys. Rev. Lett.* **77**, 3865–3868 (1996). doi:10.1103/PhysRevLett.77.3865

68. S. Grimme, S. Ehrlich, L. Goerigk, Effect of the damping function in dispersion corrected density functional theory. *J. Comput. Chem.* **32**,1456–1465 (2011). doi:10.1002/jcc.21759

69. S. Goedecker, M. Teter, Separable dual-space Gaussian pseudopotentials. *Phys. Rev. B - Condens. Matter Mater. Phys.* **54**, 1703–1710 (1996). doi:10.1103/PhysRevB.54.1703

70. J. VandeVondele, J. Hutter, Gaussian basis sets for accurate calculations on molecular systems in gas and condensed phases. *J. Chem. Phys.* **127**, 114105, 2007. doi:10.1063/1.2770708

71. M. Bonomi, G. Bussi, C. Camilloni, G. A. Tribello, P. Banáš, A. Barducci, M. Bernetti, P. G. Bolhuis, S. Bottaro, D. Branduardi, R. Capelli, P. Carloni, M. Ceriotti, A. Cesari, H. Chen, 1W. Chen, F. Colizzi, S. De, M. De La Pierre, D. Donadio, V. Drobot, B. Ensing, A. L. Ferguson, M. Filizola, J. S. Fraser, H. Fu, P. Gasparotto, F. L. Gervasio, F. Giberti, A.

Gil-Ley, T. Giorgino, G. T. Heller, G. M. Hocky, M. Iannuzzi, M. Invernizzi, K. E. Jelfs, A. Jussupow, E. Kirilin, A. Laio, V. Limongelli, K. Lindorff-Larsen, T. Löhr, F. Marinelli, L. Martin-Samos, M. Masetti, R. Meyer, A. Michaelides, C. Molteni, T. Morishita, M. Nava, C. Paissoni, E. Papaleo, M. Parrinello, J. Pfaendtner, P. Piaggi, G. Piccini, A. Pietropaolo, F. Pietrucci, S. Pipolo, D. Provasi, D. Quigley, P. Raiteri, S. Raniolo, J. Rydzewski, M. Salvalaglio, G. C. Sosso, V. Spiwok, J. Šponer, D. W. H. Swenson, P. Tiwary, O. Valsson, M. Vendruscolo, G. A. Voth, A. White, T. P. consortium, Promoting transparency and reproducibility in enhanced molecular simulations. *Nat. Methods.* **16**, 670–673 (2019). doi:10.1038/s41592-019-0506-8

72. G. A. Tribello, M. Bonomi, D. Branduardi, C. Camilloni, G. Bussi, PLUMED 2: New feathers for an old bird. *Comput. Phys. Commun.* **185**, 604–613 (2014). doi:10.1016/j.cpc.2013.09.018

73. P. Cnudde, R. Demuynck, S. Vandenbrande, M. Waroquier, G. Sastre, V. V. Speybroeck, Light Olefin Diffusion during the MTO Process on H-SAPO-34: A Complex Interplay of Molecular Factors. *J. Am. Chem. Soc.* **142**, 6007–6017 (2020). doi:10.1021/jacs.9b10249

74. Y. Sun, S. M. J. Rogge, A. Lamaire, S. Vandenbrande, J. Wieme, C. R. Siviour, V. Van Speybroeck, J.-C. Tan, High-rate nanofluidic energy absorption in porous zeolitic frameworks. *Nat. Mater.* **20**, 1015–1023 (2021). doi:10.1038/s41563-021-00977-6

75. A. Grossfield, WHAM: an implementation of the weighted histogram analysis method. http://membrane.urmc.rochester.edu/content/wham/

76. J. R. Li, R. J. Kuppler, H. C. Zhou, Selective gas adsorption and separation in metal–organic frameworks. *Chem. Soc. Rev.* **38**, 1477-1504 (2009). doi:10.1039/B802426J

77. T. D. Pham, R. F. Lobo, Adsorption equilibria of CO_2 and small hydrocarbons in AEI-, CHA-, STT-, and RRO-type siliceous zeolites. *Microporous Mesoporous Mater.* **236**, 100-108 (2016). doi:10.1016/j.micromeso.2016.08.025

78. M. J. Maple, C. D. Williams, Separating nitrogen/methane on zeolite-like molecular sieves. *Microporous Mesoporous Mater.* **111**, 627-631 (2008). doi:10.1016/j.micromeso.2007.07.014

79. R. T. Adams, J. S. Lee, T. H. Bae, J. K. Ward, J. R. Johnson, C. W. Jones, S. Nair, W. J. Koros, CO2-CH4 permeation in high zeolite 4A loading mixed matrix membranes. *J. Memb. Sci.* **367**, 197–203 (2011). doi:10.1016/j.memsci.2010.10.059

80. G. Sodeifian, M. Raji, M. Asghari, M. Rezakazemi, A. Dashti, Polyurethane-SAPO-34 mixed matrix membrane for CO2/CH4 and CO2/N2 separation. *Chinese J. Chem. Eng.* **27**, 322–334 (2019). doi:10.1016/j.cjche.2018.03.012

81. J. M. Duval, B. Folkers, M. H. V. Mulder, G. Desgrandchamps, C. A. Smolders, Adsorbent filled membranes for gas separation. Part 1. Improvement of the gas separation properties of polymeric membranes by incorporation of microporous adsorbents. *J. Memb. Sci.* **80**, 189–198 (1993). doi:10.1016/0376-7388(93)85143-K

82. L. Y. Jiang, T. S. Chung, S. Kulprathipanja, Fabrication of mixed matrix hollow fibers with intimate polymer–zeolite interface for gas separation. *AIChE J.* **52**, 2898–2908 (2006). doi:10.1002/aic.10909

83. A. Ilyas, N. Muhammad, M. A. Gilani, I. F. J. Vankelecom, A. L. Khan, Effect of zeolite

surface modification with ionic liquid [APTMS][Ac] on gas separation performance of mixed matrix membranes. *Sep. Purif. Technol.* **205**, 176–183 (2018). doi:10.1016/j.seppur.2018.05.040

84. M. U. M. Junaidi, C. P. Leo, A. L. Ahmad, S. N. M. Kamal, T. L. Chew, Carbon dioxide separation using asymmetric polysulfone mixed matrix membranes incorporated with SAPO-34 zeolite. *Fuel Process. Technol.* **118**, 125–132 (2014). doi:10.1016/j.fuproc.2013.08.009

85. M. U. M. Junaidi, C. P. Leo, S. N. M. Kamal, A. L. Ahmad, T. L. Chew, Carbon dioxide removal from methane by using polysulfone/SAPO-44 mixed matrix membranes. *Fuel Process. Technol.* **112**, 1–6 (2013). doi:10.1016/j.fuproc.2013.02.014

86. M. U. M. Junaidi, C. P. Leo, A. L. Ahmad, N. A. Ahmad, Fluorocarbon functionalized SAPO-34 zeolite incorporated in asymmetric mixed matrix membranes for carbon dioxide separation in wet gases. *Microporous Mesoporous Mater.* **206**, 23–33 (2015). doi:10.1016/j.micromeso.2014.12.013

87. Y. Li, T.S. Chung, S. Kulprathipanja, Novel Ag+-zeolite/polymer mixed matrix membranes with a high CO2/CH4 selectivity. *AIChE J.* **53**, 610-616 (2007). doi:10.1002/aic.11109

88. B. Zornoza, C. Téllez, J. Coronas, O. Esekhile, W.J. Koros, Mixed matrix membranes based on 6FDA polyimide with silica and zeolite microsphere dispersed phases. *AIChE J.* **61**, 4481-4490 (2015). doi:10.1002/aic.15011

89. M. Laghaei, M. Sadeghi, B. Ghalei, M. Shahrooz, The role of compatibility between polymeric matrix and silane coupling agents on the performance of mixed matrix membranes: Polyethersulfone/MCM-41. *J. Memb. Sci.* **513**, 20–32 (2016). doi:10.1016/j.memsci.2016.04.039

90. Y. Liu, K. Takata, Y. Mukai, H. Kita, K. Tanaka, Nano-porous Zeolite and MOF Filled Mixed Matrix Membranes for Gas Separation. *MATEC Web Conf.* **333**, 04008 (2021). doi:10.1051/matecconf/202133304008

91. S. Husain, W. J. Koros, Mixed matrix hollow fiber membranes made with modified HSSZ-13 zeolite in polyetherimide polymer matrix for gas separation. *J. Memb. Sci.* **288**, 195–207 (2007). doi:10.1016/j.memsci.2006.11.016

92. S. B. Messaoud, A. Takagaki, T. Sugawara, R. Kikuchi, S. T. Oyama, Mixed matrix membranes using SAPO-34/polyetherimide for carbon dioxide/methane separation. *Sep. Purif. Technol.* **148**, 38–48 (2015). doi:10.1016/j.seppur.2015.04.017

93. S. Shu, S. Husain, W. J. Koros, A general strategy for adhesion enhancement in polymeric composites by formation of nanostructured particle surfaces. *J. Phys. Chem. C.* **111**, 652–657 (2007). doi:10.1021/jp065711j

94. J. K. Ward, W. J. Koros, Crosslinkable mixed matrix membranes with surface modified molecular sieves for natural gas purification: I. Preparation and experimental results. *J. Memb. Sci.* **377**, 75–81 (2011). doi:10.1016/j.memsci.2011.04.010

95. A. M. W. Hillock, S. J. Miller, W. J. Koros, Crosslinked mixed matrix membranes for the purification of natural gas: Effects of sieve surface modification. *J. Memb. Sci.* **314**, 193–199 (2008). doi:10.1016/j.memsci.2008.01.046

96. O. Bakhtiari, S. Mosleh, T. Khosravi, T. Mohammadi, Preparation, Characterization and

Gas Permeation of Polyimide Mixed Matrix Membranes. *J. Membr. Sci. Technol.* **01**, 1–8 (2011). doi:10.4172/2155-9589.1000101

97. X. Y. Chen, O. G. Nik, D. Rodrigue, S. Kaliaguine, Mixed matrix membranes of aminosilanes grafted FAU/EMT zeolite and cross-linked polyimide for CO2/CH4 separation. *Polymer* **53**, 3269–3280 (2012). doi:10.1016/j.polymer.2012.03.017

98. M. Peydayesh, S. Asarehpour, T. Mohammadi, O. Bakhtiari, Preparation and characterization of SAPO-34 - Matrimid® 5218 mixed matrix membranes for CO2/CH4 separation. *Chem. Eng. Res. Des.* **91**, 1335–1342 (2013). doi:10.1016/j.cherd.2013.01.022

99. H. H. Yong, H. C. Park, Y. S. Kang, J. Won, W. N. Kim, Zeolite-filled polyimide membrane containing 2,4,6-triaminopyrimidine. *J. Memb. Sci.* **188**, 151–163 (2001). doi:10.1016/S0376-7388(00)00659-1

100. Y. Zhang, K. J. Balkus, I. H. Musselman, J. P. Ferraris, Mixed-matrix membranes composed of Matrimid® and mesoporous ZSM-5 nanoparticles. *J. Memb. Sci.* **325**, 28–39 (2008). doi:10.1016/j.memsci.2008.04.063

101. A. L. Khan, C. Klaysom, A. Gahlaut, A. U. Khan, I. F. J. Vankelecom, Mixed matrix membranes comprising of Matrimid and -SO3H functionalized mesoporous MCM-41 for gas separation. *J. Memb. Sci.* **447**, 73–79 (2013). doi:10.1016/j.memsci.2013.07.011

102. D. Carter, F. H. Tezel, B. Kruczek, H. Kalipcilar, Investigation and comparison of mixed matrix membranes composed of polyimide matrimid with ZIF–8, silicalite, and SAPO – 34. *J. Memb. Sci.* **544**, 35–46 (2017). doi:10.1016/j.memsci.2017.08.068

103. F. Dorosti, M. R. Omidkhah, M. Z. Pedram, F. Moghadam, Fabrication and characterization of polysulfone/polyimide-zeolite mixed matrix membrane for gas separation. *Chem. Eng. J.* **171**, 1469–1476 (2011). doi:10.1016/j.cej.2011.05.081

104. H. Gong, S. S. Lee, T. H. Bae, Mixed-matrix membranes containing inorganically surface-modified 5A zeolite for enhanced CO2/CH4 separation. *Microporous Mesoporous Mater.* **237**, 82–89 (2017). doi:10.1016/j.micromeso.2016.09.017

105. L. Y. Jiang, Tai S. Chung, S.Kulprathipanja, Preparation and characterization of Matrimid® 5218 based binary and ternary mixed matrix membranes for CO2 separation. *Int. J. Greenh. Gas Control*. **39**, 225–235 (2015). doi:10.1016/j.ijggc.2015.04.016

106. A. E. Amooghin, M. Omidkhah, H. Sanaeepur, A. Kargari, Preparation and characterization of Ag+ ion-exchanged zeolite-Matrimid®5218 mixed matrix membrane for CO2/CH4 separation. *J. Energy Chem.* **25**, 450–462 (2016). doi:10.1016/j.jechem.2016.02.004

107. A. Ebadi Amooghin, M. Omidkhah, A. Kargari, Enhanced CO2 transport properties of membranes by embedding nano-porous zeolite particles into Matrimid®5218 matrix. *RSC Adv.* **5**, 8552–8565 (2015). doi:10.1039/c4ra14903c

108. A. E. Amooghin, H. Sanaeepur, M. Omidkhah, A. Kargari, "Ship-in-a-Bottle", a New Synthesis Strategy for Preparing Novel Hybrid Host-Guest Nanocomposites for Highly Selective Membrane Gas Separation. *J. Mater. Chem. A.* **6**, 1751–1771 (2018). doi:10.1039/c7ta08081f

109. J. Zhao, K. Xie, L. Liu, M. Liu, W. Qiu, P. A. Webley, Enhancing plasticization-resistance of mixed-matrix membranes with exceptionally high CO2/CH4 selectivity through incorporating ZSM-25 zeolite. *J. Memb. Sci.* **583**, 23–30 (2019).

doi:10.1016/j.memsci.2019.03.073

110. Z. Tahir, A. Ilyas, X. Li, M. R. Bilad, I. F. J. Vankelecom, A. L. Khan, Tuning the gas separation performance of fluorinated and sulfonated PEEK membranes by incorporation of zeolite 4A. *J. Appl. Polym. Sci.* **135** (2018). doi:10.1002/app.45952

111. M.Z. Ahmad, V. Martin-Gil, T. Supinkova, P. Lambert, R. Castro-Muñoz, P. Hrabanek, M. Kocirik, V. Fila, Novel MMM using CO2 selective SSZ-16 and high-performance 6FDA-polyimide for CO2/CH4 separation. *Sep. Purif. Technol*. **254**, 117582 (2021), doi:10.1016/j.seppur.2020.117582

112. T. Wu, Y. Shi, Y. Liu, I. Kumakiri, K. Tanaka, X. Chen, H. Kita, Improved Gas Permeation Properties of 6FDA-TrMPD Mixed-Matrix Membrane with SAPO-34 Crystals Toward CO2 Separation. *Energy and Fuels*. **35**, 10680–10688 (2021). doi:10.1021/acs.energyfuels.1c00925

113. T. W. Pechar, S. Kim, B. Vaughan, E. Marand, V. Baranauskas, J. Riffle, H. K. Jeong, M. Tsapatsis, Preparation and characterization of a poly(imide siloxane) and zeolite L mixed matrix membrane. *J. Memb. Sci.* **277**, 210–218 (2006). doi:10.1016/j.memsci.2005.10.031

114. S. Escorihuela, L. Valero, A. Tena, S. Shishatskiy, S. Escolástico, T. Brinkmann, J. M. Serra, Study of the effect of inorganic particles on the gas transport properties of glassy polyimides for selective CO2 and H2O separation. *Membranes (Basel).* **8** (2018). doi:10.3390/membranes8040128

115. H. Sanaeepur, A. Kargari, B. Nasernejad, Aminosilane-functionalization of a nanoporous Y-type zeolite for application in a cellulose acetate based mixed matrix membrane for CO2 separation. *RSC Adv.* **4**, 63966–63976 (2014). doi:10.1039/c4ra08783f

116. H. Sanaeepur, A. Kargari, B. Nasernejad, A. Ebadi Amooghin, M. Omidkhah, A novel Co2+ exchanged zeolite Y/cellulose acetate mixed matrix membrane for CO2/N2 separation. *J. Taiwan Inst. Chem. Eng.* **60**, 403–413 (2016). doi:10.1016/j.jtice.2015.10.042

117. H. Sanaeepur, A. Ebadi Amooghin, A. Kargari, M. Omidkhah, A. Fauzi Ismail, S. Ramakrishna, Interior Modification of Nano-Porous Fillers to Fabricate High Performance Mixed Matrix Membranes. *Iran. J. Chem. Eng.* **16**, 70–94 (2019). http://www.ijche.com/article_90036.html%0Ahttp://www.ijche.com/article_90036_6756757b92e2a372b4f2d8334f5cd660.pdf

118. J. Ahmad, M. B. Hägg, Development of matrimid/zeolite 4A mixed matrix membranes using low boiling point solvent. *Sep. Purif. Technol.* **115**, 190–197 (2013). doi:10.1016/j.seppur.2013.04.049

119. C. I. Chaidou, G. Pantoleontos, D. E. Koutsonikolas, S. P. Kaldis, G. P. Sakellaropoulos, Gas Separation Properties of Polyimide-Zeolite Mixed Matrix Membranes. *Sep. Sci. Technol.* **47**, 950–962 (2012). doi:10.1080/01496395.2011.645263

120. Y. Wang, Y. Zhou, X. Zhang, Y. Gao, J. Li, SPEEK membranes by incorporation of NaY zeolite for CO2/N2 separation. *Sep. Purif. Technol.* **275**, 119189 (2021). doi:10.1016/j.seppur.2021.119189

121. M. G. Süer, N. Baç, L. Yilmaz, Gas permeation characteristics of polymer-zeolite mixed matrix membranes. *J. Memb. Sci.* **91**, 77–86 (1994). doi:10.1016/0376-7388(94)00018-2

122. J. Yu, L. Li, N. Liu, R. Lee, An approach to prepare defect-free PES/MFI-type zeolite mixed

matrix membranes for CO2/N2 separation. *J. Mater. Sci.* **48**, 3782–3788 (2013). doi:10.1007/s10853-013-7178-z

123. Y. Yu, C. Zhang, J. Fan, D. Liu, J. Meng, A mixed matrix membrane for enhanced CO2/N2 separation via aligning hierarchical porous zeolite with a polyethersulfone based comb-like polymer. *J. Taiwan Inst. Chem. Eng.* **132,** (2022). doi:10.1016/j.jtice.2021.10.032

124. T. M. Gür, Permselectivity of zeolite filled polysulfone gas separation membranes. *J. Memb. Sci.* **93**, 283–289 (1994). doi:10.1016/0376-7388(94)00102-2

125. N. N. R. Ahmad, C. P. Leo, A. W. Mohammad, A. L. Ahmad, Interfacial sealing and functionalization of polysulfone/SAPO-34 mixed matrix membrane using acetate-based ionic liquid in post-impregnation for CO2 capture. *Sep. Purif. Technol.* **197**, 439–448 (2018). doi:10.1016/j.seppur.2017.12.054

126. A. Jomekian, M. Pakizeh, S. A. A. Mansoori, M. Poorafshari, M. Hemmati, D. P. Ataee, Gas transport behavior of novel modified MCM-48/ polysulfone mixed matrix membrane coated by PDMS. *J. Membra. Sci. Technol.* **1**, 102 (2011). doi:10.4172/2155-9589.1000102

127. B. Zornoza, B. Seoane, J. M. Zamaro, C. Téllez, J. Coronas, Combination of MOFs and zeolites for mixed-matrix membranes. *ChemPhysChem*. **12**, 2781–2785 (2011). doi:10.1002/cphc.201100583

128. P. Natarajan, B. Sasikumar, S. Elakkiya, G. Arthanareeswaran, A. F. Ismail, W. Youravong, E. Yuliwati, Pillared cloisite 15A as an enhancement filler in polysulfone mixed matrix membranes for CO2/N2 and O2/N2 gas separation. *J. Nat. Gas Sci. Eng.* **86**, 103720 (2021). doi:10.1016/j.jngse.2020.103720

129. A. Fernández-Barquín, R. Rea, D. Venturi, M. Giacinti-Baschetti, M. G. De Angelis, C. Casado-Coterillo, Á. Irabien, Effect of relative humidity on the gas transport properties of zeolite A/PTMSP mixed matrix membranes. *RSC Adv.* **8**, 3536–3546 (2018). doi:10.1039/c7ra13039b

130. H. T. Afarani, M. Sadeghi, A. Moheb, The Gas Separation Performance of Polyurethane–Zeolite Mixed Matrix Membranes. *Adv. Polym. Technol.* **37**, 339–348 (2018). doi:10.1002/adv.21672

131. M. S. A. Wahab, A. R. Sunarti, Production of Mixed Matrix (PVDF/Zeolite) Membrane for CO2/N2 Gas Separation. *Int. J. Chem. Biomol. Sci.* **1**, 264–270 (2015). http://www.aiscience.org/journal/ijcbshttp://creativecommons.org/licenses/by-nc/4.0/

132. Y. Shen, A. C. Lua, Preparation and characterization of mixed matrix membranes based on poly(vinylidene fluoride) and zeolite 4A for gas separation. *Polym. Eng. Sci.* **52**, 2106–2113 (2012). doi:10.1002/pen.23165

133. M. L. Carreon, S. Li, M. A. Carreon, AlPO-18 membranes for CO2/CH4 separation. *Chem. Commun.* **48**, 2310–2312 (2012). doi:10.1039/c2cc17249f

134. T. Wu, B. Wang, Z. Lu, R. Zhou, X. Chen, Alumina-supported AlPO-18 membranes for CO2/CH4 separation. *J. Memb. Sci.* **471**, 338–346 (2014). doi:10.1016/j.memsci.2014.08.035

135. B. Wang, N. Hu, H. Wang, Y. Zheng, R. Zhou, Improved AlPO-18 membranes for light gas separation. *J. Mater. Chem. A.* **3**, 12205–12212 (2015). doi:10.1039/c5ta01260k

136. S. Zhong, N. Bu, R. Zhou, W. Jin, M. Yu, S. Li, Aluminophosphate-17 and silicoaluminophosphate-17 membranes for CO2 separations. *J. Memb. Sci.* **520**, 507–514 (2016). doi:10.1016/j.memsci.2016.08.010

137. N. Kosinov, C. Auffret, V. G. P. Sripathi, C. Gücüyener, J. Gascon, F. Kapteijn, E. J. M. Hensen, Influence of support morphology on the detemplation and permeation of ZSM-5 and SSZ-13 zeolite membranes. *Microporous Mesoporous Mater.* **197**, 268–277 (2014). doi:10.1016/j.micromeso.2014.06.022

138. Y. Zheng, N. Hu, H. Wang, N. Bu, F. Zhang, R. Zhou, Preparation of steam-stable high-silica CHA (SSZ-13) membranes for CO2/CH4 and C2H4/C2H6 separation. *J. Memb. Sci.* **475**, 303–310 (2015). doi:10.1016/j.memsci.2014.10.048

139. B. Wang, Y. Zheng, J. Zhang, W. Zhang, F. Zhang, W. Xing, R. Zhou, Separation of light gas mixtures using zeolite SSZ-13 membranes. *Microporous Mesoporous Mater.* **275**, 191–199 (2019). doi:10.1016/j.micromeso.2018.08.032

140. K. Kida, Y. Maeta, K. Yogo, Preparation and gas permeation properties on pure silica CHA-type zeolite membranes. *J. Memb. Sci.* **522**, 363–370 (2017). doi:10.1016/j.memsci.2016.09.00251

141. R. Zhou, E. W. Ping, H. H. Funke, J. L. Falconer, R. D. Noble, Improving SAPO-34 membrane synthesis. *J. Memb. Sci.* **444**, 384–393 (2013). doi:10.1016/j.memsci.2013.05.048

142. S. Li, J. L. Falconer, R. D. Noble, Improved SAPO-34 membranes for CO2/CH4 separations. *Adv. Mater.* **18**, 2601–2603 (2006). doi:10.1002/adma.200601147

143. Y. Hasegawa, T. Tanaka, K. Watanabe, B. H. Jeong, K. Kusakabe, S. Morooka, Separation of CO2-CH4 and CO2-N2 Systems Using Ion-exchanged FAU-type Zeolite Membranes with Different Si/Al Ratios. *Korean J. Chem. Eng.* **19**, 309–313 (2002). doi:10.1007/BF02698420

144. K. Kusakabe, T. Kuroda, A. Murata, S. Morooka, Formation of a Y-Type Zeolite Membrane on a Porous α-Alumina Tube for Gas Separation. *Ind. Eng. Chem. Res.* **36**, 649–655 (1997). doi:10.1021/ie960519x

145. J. Van Den Bergh, W. Zhu, F. Kapteijn, J. A. Moulijn, K. Yajima, K. Nakayama, T. Tomita, S. Yoshida, Separation of CO2 and CH4 by a DDR membrane. *Res. Chem. Intermed.* **34**, 467–474 (2008). doi:10.1163/156856708784795680

146. S. Himeno, T. Tomita, K. Suzuki, K. Nakayama, K. Yajima, S. Yoshida, Synthesis and permeation properties of a DDR-type zeolite membrane for separation of CO2/CH4 gaseous mixtures. *Ind. Eng. Chem. Res.* **46**, 6989–6997 (2007). doi:10.1021/ie061682n

147. N. Xu, D. Meng, X. Tang, X. Kong, L. Kong, Y. Zhang, H. Qiu, M. Wang, Y. Zhang, Fast synthesis of thin all-silica DDR zeolite membranes with inorganic base as mineralizing agent for CO2/CH4 separation. *Sep. Purif. Technol.* **253**, 117505 (2020). doi:10.1016/j.seppur.2020.117505

148. M. Sen, K. Dana, N. Das, Development of LTA zeolite membrane from clay by sonication assisted method at room temperature for H2-CO2 and CO2-CH4 separation. *Ultrason. Sonochem.* **48**, 299–310 (2018). doi:10.1016/j.ultsonch.2018.06.007

149. L. Yu, S. Fouladvand, M. Grahn, J. Hedlund, Ultra-thin MFI membranes with different

Si/Al ratios for CO2/CH4 separation. *Microporous Mesoporous Mater.* **284**, 258–264 (2019). doi:10.1016/j.micromeso.2019.04.042

150. H. Guo, G. Zhu, H. Li, X. Zou, X. Yin, W. Yang, S. Qiu, R. Xu, Hierarchical growth of large-scale ordered zeolite silicalite-1 membranes with high permeability and selectivity for recycling CO2. *Angew. Chemie - Int. Ed.* **45**, 7053–7056 (2006). doi:10.1002/anie.200602308

151. B. Wang, Y. Wang, X. Li, S. Zhong, R. Zhou, Highly CO2-selective and moisture-resistant bilayer silicalite-1/SSZ-13 membranes with gradient pores for wet CO2/CH4 and CO2/N2 separations. *J. Memb. Sci.* **636**, 119565 (2021). doi:10.1016/j.memsci.2021.119565

152. E. Beerdsen, B. Smit, and D. Dubbeldam, Molecular Simulation of Loading Dependent Slow Diffusion in Confined Systems. *Phys. Rev. Lett.* **93**, 248301, (2004). doi:10.1103/PhysRevLett.93.248301

153. X. J. Gu, Raman spectroscopy and the effects of ultraviolet irradiation on polyimide film. *Appl. Phys. Lett.* **62**, 1568–1570 (1993). doi:10.1063/1.108643

154. B. A. Kolesov, Hydrogen bonds: Raman spectroscopic study. *Int. J. Mol. Sci.* **22,** (2021). doi:10.3390/ijms22105380

155. P. Bock, N. Gierlinger, Infrared and Raman spectra of lignin substructures: Coniferyl alcohol, abietin, and coniferyl aldehyde. *J. Raman Spectrosc.* **50**, 778–792 (2019). doi:10.1002/jrs.5588

156. J. Shang, G. Li, R. Singh, Q. Gu, K. M. Nairn, T. J. Bastow, N. Medhekar, C. M. Doherty, A. J. Hill, J. Z. Liu, P. A. Webley, Discriminative separation of gases by a "molecular trapdoor" mechanism in chabazite zeolites. *J. Acm. Chem. Soc.* **134**, 19246–19253 (2012). doi:10.1021/ja309274y

157. H. Vinh-Thang, S. Kaliaguine, Predictive models for mixed-matrix membrane performance: A review. *Chem. Rev.* **113**, 4980–5028 (2013). doi:10.1021/cr3003888

158. Y. Han, Y. Yang, W. S. Winston Ho, Recent progress in the engineering of polymeric membranes for CO2 capture from flue gas. *Membranes (Basel).* **10**, 1–35 (2020). doi:10.3390/membranes10110365

159. T. D. Pham, M. R. Hudson, C. M. Brown, R. F. Lobo, Molecular basis for the high CO2 adsorption capacity of chabazite zeolites. *ChemSusChem*. **7**, 3031–3038 (2014). doi:10.1002/cssc.201402555

160. D. H. Olson, M. A. Camblor, L. A. Villaescusa, G. H. Kuehl, Light hydrocarbon sorption properties of pure silica Si-CHA and ITQ-3 and high silica ZSM-58. *Microporous Mesoporous Mater.* **67**, 27–33 (2004). doi:10.1016/j.micromeso.2003.09.025

161. Y. Li, H. Yi, X. Tang, F. Li, Q. Yuan, Adsorption separation of CO2/CH4 gas mixture on the commercial zeolites at atmospheric pressure. *Chem. Eng. J.* **229**, 50–56 (2013). doi:10.1016/j.cej.2013.05.101

162. M. Palomino, A. Corma, J. L. Jordà, F. Rey, S. Valencia, Zeolite Rho: A highly selective adsorbent for CO2/CH4 separation induced by a structural phase modification. *Chem. Commun.* **48**, 215–217 (2012). doi:10.1039/c1cc16320e

163. N. Ghasem, CO2 removal from natural gas. *Adv. Carbon Capture*, 479–501 (2020).

doi:10.1016/b978-0-12-819657-1.00021-9

164. Y. Hasegawa, C. Abe, T. Ikeda, K. Sato, Influence of change in the unit cell parameters on permeation properties of AEI-type zeolite membrane. *J. Memb. Sci.* **499**, 538–543 (2016). doi:10.1016/j.memsci.2015.11.020

165. Y. W. Jeon, D. H. Lee, Gas membranes for CO2/CH4 (biogas) separation: A review. *Environ. Eng. Sci.* **32**, 71–85 (2015). doi:10.1089/ees.2014.0413

166. G. Liu, A. Cadiau, Y. Liu, K. Adil, V. Chernikova, I. D. Carja, Y. Belmabkhout, M. Karunakaran, O. Shekhah, C. Zhang, A. K. Itta, S. Yi, M. Eddaoudi, W. J. Koros, Enabling Fluorinated MOF-Based Membranes for Simultaneous Removal of H2S and CO2 from Natural Gas. *Angew. Chemie - Int. Ed.* **57**, 14811–14816 (2018). doi:10.1002/anie.201808991

167. M. M. Lozinska, E. Mangano, J. P. S. Mowat, A. M. Shepherd, R. F. Howe, S. P. Thompson, J. E. Parker, S. Brandani, P. A. Wright, Understanding carbon dioxide adsorption on univalent cation forms of the flexible zeolite Rho at conditions relevant to carbon capture from flue gases. *J. Am. Chem. Soc.* **134**, 17628–17642 (2012). doi:10.1021/ja3070864

168. Z. X. Low, P. M. Budd, N. B. McKeown, D. A. Patterson, Gas permeation properties, physical aging, and its mitigation in high free volume glassy polymers. *Chem. Rev.* **118**, 5871–5911 (2018). doi:10.1021/acs.chemrev.7b00629

169. A. de J. Montes Luna, G. Castruita de León, S. P. García Rodríguez, N. C. Fuentes López, O. Pérez Camacho, Y. A. Perera Mercado, Na+/Ca2+ aqueous ion exchange in natural clinoptilolite zeolite for polymer-zeolite composite membranes production and their CH4/CO2/N2 separation performance. *J. Nat. Gas Sci. Eng.* **54**, 47–53 (2018). doi:10.1016/j.jngse.2018.03.007

170. M. Miyamoto, Y. Fujioka, K. Yogo, Pure silica CHA type zeolite for CO2 separation using pressure swing adsorption at high pressure. *J. Mater. Chem.* **22**, 20186–20189 (2012). doi:10.1039/c2jm34597h

171. F. Hirosawa, M. Miyagawa, H. Takaba, Selectivity enhancement by the presence of grain boundary in chabazite zeolite membranes investigated by non-equilibrium molecular dynamics. *J. Memb. Sci.* **632**, 119348 (2021). doi:10.1016/j.memsci.2021.119348

172. R. Mahajan, W. J. Koros, Mixed matrix membrane materials with glassy polymers. Part 1. *Polym. Eng. Sci.* **42**, 1420–1431 (2002). doi:10.1002/pen.11041

173. R. Mahajan, W. J. Koros, Mixed matrix membrane materials with glassy polymers. Part 2. *Polym. Eng. Sci.* **42**, 1432–1441 (2002). doi:10.1002/pen.11042

174. R. Castro-Muñoz, V. Fíla, Progress on incorporating zeolites in matrimid® 5218 mixed matrix membranes towards gas separation. *Membranes (Basel).* **8**, 1–23 (2018). doi:10.3390/membranes8020030

175. M. Carreon, G. Dahe, J. Feng, S. R. Venna, Mixed matrix membranes for gas separation applications. *Membr. Gas Sep.*, 1–58 (2017). doi:10.1142/9789813207714_0001

176. T. S. Chung, L. Y. Jiang, Y. Li, S. Kulprathipanja, Mixed matrix membranes (MMMs) comprising organic polymers with dispersed inorganic fillers for gas separation. *Prog. Polym. Sci.* **32**, 483–507 (2007). doi:10.1016/j.progpolymsci.2007.01.008

177. L. M. Robeson, Z. P. Smith, B. D. Freeman, D. R. Paul, Contributions of diffusion and solubility selectivity to the upper bound analysis for glassy gas separation membranes. *J. Memb. Sci.* **453**, 71–83 (2014). doi:10.1016/j.memsci.2013.10.066

178. L. Y. Jiang, T. S. Chung, C. Cao, Z. Huang, S. Kulprathipanja, Fundamental understanding of nano-sized zeolite distribution in the formation of the mixed matrix single- and dual-layer asymmetric hollow fiber membranes. *J. Memb. Sci.* **252**, 89–100 (2005). doi:10.1016/j.memsci.2004.12.004

179. C. A. Dunn, S. Denning, J. M. Crawford, R. Zhou, G. E. Dwulet, M. A. Carreon, D. L. Gin, R. D. Noble, CO2/CH4 separation characteristics of poly(RTIL)-RTIL-zeolite mixed-matrix membranes evaluated under binary feeds up to 40 bar and 50°C. *J. Memb. Sci.* **621**, 118979 (2021). doi:10.1016/j.memsci.2020.118979

180. R. Nasir, N. N. R. Ahmad, H. Mukhtar, D. F. Mohshim, Effect of ionic liquid inclusion and amino-functionalized SAPO-34 on the performance of mixed matrix membranes for CO2/CH4 separation. *J. Environ. Chem. Eng.* **6**, 2363–2368 (2018). doi:10.1016/j.jece.2018.03.032

181. C. Casado-Coterillo, A. Fernández-Barquín, S. Valencia, Á. Irabien, Estimating CO2/N2 permselectivity through Si/Al = 5 small-pore zeolites/PTMSP mixed matrix membranes: Influence of temperature and topology. *Membranes (Basel).* **8** (2018). doi:10.3390/membranes8020032

182. G. L. Zhuang, H. H. Tseng, M. Y. Wey, Preparation of PPO-silica mixed matrix membranes by in-situ sol-gel method for H2/CO2 separation. *Int. J. Hydrogen Energy*. **39**, 17178–17190 (2014). doi:10.1016/j.ijhydene.2014.08.050

183. Y. Li, T. S. Chung, C. Cao, S. Kulprathipanja, The effects of polymer chain rigidification, zeolite pore size and pore blockage on polyethersulfone (PES)-zeolite A mixed matrix membranes. *J. Memb. Sci.* **260**, 45–55 (2005). doi:10.1016/j.memsci.2005.03.019

184. M. Peydayesh, T. Mohammadi, O. Bakhtiari, Effective hydrogen purification from methane via polyimide Matrimid® 5218- Deca-dodecasil 3R type zeolite mixed matrix membrane. *Energy*. **141**, 2100–2107 (2017). doi:10.1016/j.energy.2017.11.101

185. L. Hu, J. Cheng, Y. Li, J. Liu, L. Zhang, J. Zhou, K. Cen, Composites of ionic liquid and amine-modified SAPO-34 improve CO2 separation of CO2-selective polymer membranes. *Appl. Surf. Sci.* **410**, 249–258 (2017). doi:10.1016/j.apsusc.2017.03.045

186. J. A. S. Costa, V. H. V. Sarmento, L. P. C. Romão, C. M. Paranhos, Removal of polycyclic aromatic hydrocarbons from aqueous media with polysulfone/MCM-41 mixed matrix membranes. *J. Memb. Sci.* **601** (2020). doi: 0.1016/j.memsci.2020.117912

187. K. Nematolahi, E. Salehi, A. Ebadi Amooghin, H. Sanaeepur, CO2 separation of a novel Ultem-based mixed matrix membrane incorporated with Ni2+-exchanged zeolite X. *Greenh. Gases Sci. Technol.* **12**, 48–66 (2022). doi:10.1002/ghg.2122

188. A. Mundstock, S. Friebe, J. Caro, On comparing permeation through Matrimid®-based mixed matrix and multilayer sandwich FAU membranes: H2/CO2 separation, support functionalization and ion exchange. *Int. J. Hydrogen Energy*. **42**, 279–288 (2017). doi:10.1016/j.ijhydene.2016.10.161

189. Y. Chen, L. Zhao, B. Wang, P. Dutta, W. S. Winston Ho, Amine-containing polymer/zeolite

Y composite membranes for CO2/N2 separation. *J. Memb. Sci.* **497**, 21–28 (2016). doi:10.1016/j.memsci.2015.09.036

190. A. H. McMillan, J. Mora-Macías, J. Teyssandier, R. Thür, E. Roy, I. Ochoa, S. D. Feyter, I. F. J. Vankelecom, M. B. J. Roeffaers, S. C. Lesher-Pérez, Self-sealing thermoplastic fluoroelastomer enables rapid fabrication of modular microreactors. *Nano Select.* **2**, 1385-1402 (2021). doi:10.1002/nano.202000241

191. K. M. Rodriguez, W. Wu, T. Alebrahim, Y. Cao, B. D. Freeman, D. Harrigan, M. Jhalaria, A. Kratochvil, S. Kumar, W. H. Lee, Y. M. Lee, H. Lin, J. M. Richardson, Q. Song, B. Sundell, R. Thür, I. Vankelecom, A. Wang, L. Wang, C. Wiscount, Z. P. Smith, Multi-lab study on the pure-gas permeation of commercial polysulfone (PSf) membranes: Measurement standards and best practices. *J. Memb. Sci.* **659**, 120746 (2022). doi:10.1016/j.memsci.2022.120746

Acknowledgments: We thank Maarten Roeffaers (KU Leuven, cMACS) for providing the Raman Spectromicroscopy measurement, and Maarten Bastin for density measurement. This work was supported by the Fund for Scientific Research Flanders (FWO) and the Research Board of Ghent University (BOF). The computational resources (Stevin Supercomputer Infrastructure) and services used in this work were provided by the VSC (Flemish Supercomputer Center), funded by Ghent University, FWO, and the Flemish Government – department EWI.

Funding:

Strategic Basic Research, Research Foundation - Flanders “SBOFWO” Biogas-Mambo S003721N (Xiaoyu Tan, Ivo Vankelecom)

VlaioCataSPC moonrise HBC.2020.2612 (Xiaoyu Tan, Ivo Vankelecom)

Research Foundation – Flanders “FWO” scholarship: 1241822N, 12X7319N, 1SB8821N (Raymond Thür, Yun Li, Daan Van Havere)

Research Foundation – Flanders “FWO” G085220N (Sven Robijns, Niels De Witte, Tom Van Assche, Michiel Dusselier)

Hercules fund AKUL/13/19 (Ivo Vankelecom)

Author contributions:

Conceptualization: Xiaoyu Tan, Quanli Ke, Ivo Vankelecom.

Methodology: Xiaoyu Tan, Sven Robijns, Quanli Ke, Raymond Thür, Michiel Dusselier, Ivo Vankelecom.

Investigation: Xiaoyu Tan, Sven Robijns, Quanli Ke, Niels De Witte, Aran Lamaire, Yun Li, Imran Aslam, Daan Van Havere, Thibaut Donckels.

Visualization: Xiaoyu Tan, Sven Robijns, Aran Lamaire, Niels De Witte.

Funding acquisition: Ivo Vankelecom, Michiel Dusselier, Tom Van Assche, Veronique Van Speybroeck.

Project administration: Xiaoyu Tan, Ivo Vankelecom.

Supervision: Ivo Vankelecom.

Writing – original draft: Xiaoyu Tan, Raymond Thür.

Writing – review & editing: All authors.

Competing interests: Authors declare that they have no competing interests. Xiaoyu Tan, Ivo Vankelecom, Michiel Dusselier, Sven Robijns, Raymond Thür submitted patent application EP22170367.1 by KU Leuven based on this invention.

Data and materials availability: All data are available in the main text or the supplementary materials.

Supplementary Materials

Materials and Methods

Supplementary Text

Figs. S1 to S66

Tables S1 to S21

References (*43*-*191*)

Movies S1 to S2

Data S1